Applied Clay Science 88–89 (2014) 26–32

Contents lists available at ScienceDirect

Applied Clay Science

journal homepage: www.elsevier.com/locate/clay

Research paper

Some consequences of the fluorination of brucite-like layers in layered double hydroxides: Adsorption

Enrique Lima [a,*], Heriberto Pfeiffer [a], Jorge Flores [b]

[a] Instituto de Investigaciones en Materiales, Universidad Nacional Autónoma de Mexico, Circuito exterior s/n, Cd. Universitaria, Del. Coyoacán, CP 04510, Mexico D.F., Mexico
[b] Universidad Autónoma Metropolitana, Azcapotzalco, Av. San Pablo 180, Col. Reynosa Tamaulipas, 02200 Mexico D.F., Mexico

ARTICLE INFO

Article history:
Received 9 June 2013
Received in revised form 10 December 2013
Accepted 12 December 2013
Available online 5 January 2014

Keywords:
Hydrotalcite
Layered double hydroxides
Adsorption
Fluorine

ABSTRACT

Hydrotalcite-like compounds were synthesised by co-precipitation method. The originality of the work is the replacement of structural OH^- by F^-. Fluoride anions were incorporated as a part of the brucite like layers not as compensating anions. The resulting adsorptive properties of fluorinated materials are very different than those observed for the fluorine-free sample. The polarity and polarisability parameters were calculated by using dyes and xenon as molecular probes. The hydrogen bond accepting character and acido-basicity are the main properties enhanced because of the fluorination of hydrotalcite-like compounds, helping to diversify adsorption sites for chromophores or water.

1. Introduction

Layered double hydroxides (LDHs), commonly called hydrotalcite-like compounds (HTs), are a family of compounds currently used as catalysts, catalyst supports, adsorbents and ionic exchangers (Hattori, 1995; Laguna et al., 2007; Occelli et al., 2003; Perioli et al., 2011).

The versatility of LDHs is a consequence of their chemical structure that can be derived from a brucite structure ($Mg(OH)_2$), which is composed of linked octahedrons of magnesium hydroxide. The octahedrons form gibbsite-type sheets stacked in a hexagonal space group (Duan and Evans, 2006). In LDHs, a fraction of the divalent Mg^{2+} ions is substituted by trivalent cations, *e.g.*, Al^{3+}. Because of this substitution, the hydroxide layers become positively charged but are charge-compensated by interlayer anions or anionic complexes. The composition of LDHs is described by the formula $[M^{2+}_{1-x}M^{3+}_x(OH)_2][A^{n-}]_{x/n}.mH_2O$, where M^{2+} and M^{3+} are the di- and trivalent cations in the octahedral positions within the hydroxide layers. The value of x commonly ranges from 0.17 to 0.33. A^{n-} represents an exchangeable interlayer anion that can vary. Although LDHs show the greatest affinity by carbonates, other anionic species can also intercalate into the space between the layers (Beaudot et al., 2004; Costantino et al., 1999; Miyata, 1975). The M^{3+} and M^{2+} ions are often Al^{3+} and Mg^{2+}, respectively but may also be one of following: Ga^{3+}, Cr^{3+}, Fe^{3+}, Ni^{2+}, Zn^{2+}, and Cu^{2+} among others.

Chemical composition variation is the best strategy to tune the acid–base properties of LDHs. In this sense, the nature of M^{3+} and M^{2+} has been widely explored (Cheng et al., 2011; Sampieri and Lima, 2009). However, the replacement of structural hydroxyl by fluoride was just reported last year (Lima et al., 2012). XRD and NMR results supported the replacement of blocks $(Al(OH)_6)^{3-}$ by $(AlF_6)^{3-}$. Fluorination of hydroxide layers changes significantly the physicochemical properties of LDHs; notably, the presence of fluoride diversifies the strength and number of acid–base pairs, as supported by qualitative and quantitative analyses of probe molecule adsorption, CH_3NO_2 (nitromethane) and NH_3 (ammonia), respectively.

The layered structure of LDHs collapses due to dehydration, dehydroxylation and anion loss when LDH is treated at temperatures between 200 and 400 °C. When this collapse occurs, mixed oxides are often obtained, which are commonly able to recover the layered structure when put in contact with water or an anionic aqueous solution. The collapse-recovery of the layered structure is frequently referred to as the "memory effect" (Pfeiffer et al., 2010; Stanimirova et al., 1999; Xu and Zeng, 2001). This effect is a property of the fluorine-free LDHs as well as of the fluorinated LDHs; obviously the presence of fluorine affects the cycle collapse-recovery of the layered structure. Particularly, during calcination, the coordination of M^{3+} ions is partially lowered from octahedral to tetrahedral with the presence of fluorine enhancing the tetrahedral/octahedral ratio (Hibino and Tsunashima, 1998; Martínez-Ortiz et al., 2008). Therefore, the textural and structural properties of the fluorinated LDHs become different from those of the fluorine-free LDH. Thus, the goal of this work is to show some of the adsorptive properties of LDHs that are greatly influenced by the fluorination. The objective of many approaches is to determine the influence of fluorination on the hydrogen bond accepting character and on the acido-basicity of the mixed oxides. The modification of the nature of adsorption sites was on one hand probed by the modulation of adsorption

* Corresponding author. Tel.: +52 55 5622 4640; fax: +52 55 5616 1371.
E-mail address: lima@iim.unam.mx (E. Lima).

0169-1317/$ – see front matter © 2013 Elsevier B.V. All rights reserved.
http://dx.doi.org/10.1016/j.clay.2013.12.011

of hydroxynaphthol blue (HNB) as pigment and H_2O and CO_2 in gas phase. On the other hand, polarity and polarisability of the surface (Katritzky et al., 2004; Seifert et al., 2012; Zimmermann et al., 2002) were investigated by NMR *via* the adsorption of Xe and by UV–vis spectroscopy *via* the adsorption of a series of solvatochromic dyes.

2. Experimental procedure

2.1. Materials

Carbonate-containing Mg–Al LDHs with a Mg/Al molar ratio close to 3 were prepared by co-precipitation method at pH 10. A 1 M aqueous solution containing appropriate amounts of $Mg(NO_3)_2 \cdot 6H_2O$, $Al(NO_3)_3 \cdot 9H_2O$ and Na_3AlF_6 (Aldrich, 99.99%, USA) was delivered into a reactor by a chromatographic pump at a constant flow of 1 cm^3/min. A second aqueous solution containing 2.0 M NaOH (Aldrich, 99%) plus 0.2 M Na_2CO_3 was simultaneously fed. The pH remained constant by controlling the addition of the alkaline solution using a pH-STAT Titrando apparatus (Metrohm, Switzerland). The suspension was stirred overnight at 80 °C, and then the solid was separated by centrifugation, rinsed thoroughly with distilled water, and dried overnight at 80 °C. The ratio of Mg/Al was maintained at 3 in the samples reported in this work. The source of aluminium was either aluminium nitrate or a mixture of aluminium nitrate with sodium hexafluoro-aluminate. A series varying the amount of fluorine was prepared. Table 1 summarises the composition of four samples under study.

2.2. Adsorption

Several molecules, polar or non polar, were adsorbed either from a gas or a liquid phase in order to show the different adsorptive properties of LDH with and without fluorine. Before the adsorption tests, the adsorbents were thermal treated at 400 °C for 8 h.

2.2.1. Dyes

The following dyes were used with the purpose to evaluate the polarity parameters of mixed oxides emerged from thermal treatment of LDHs: dicyano-bis-(1,10-phenanthroline)-iron(II) complex (**1**); 3-(4-amino-3-methylphenyl)-7-phenyl-benzo-[1,2-b:4,5-b0]-difuran-2,6-dione (**2**) and 4-tert-butyl-2-(dicyano-methylene)-5-[4-(diethylamino) benzylidene]-Δ-thiazoline (**3**), Scheme 1. Adsorption of dyes was done according to the procedure followed earlier (Lungwitz and Spange, 2008; Spange et al., 2005). Briefly, dyes **2** and **3** were dissolved in cyclohexane, dye **1** was dissolved in dichloromethane. 5 mL of the dye solution per 0.1 g of the mixed oxide powder was used. The suspensions were shaken for 15 min under exclusion of light, decanted and dried under vacuum.

The evaluation of the polarity of samples was determined by monitoring solvent-dependent shifts of the UV/vis absorption band of a probe dye resulting from both rather specific (hydrogen bond donating (HBD) and hydrogen bond accepting (HBA)) and non-specific interactions (dipole–dipole, dipole–induced dipole, or London dispersion forces). In this sense, the multi-parameter approach of Kamlet–Taft was used to determine polarity of "white" oxide surfaces (Spange et al., 1999, 2001, 2005).

Table 1
Chemical composition of LDH samples synthesised by co-precipitation method.

Code Sample	Chemical formula[a]	Mg/Al ratio	d_{003} (Å)[b]
MA	$[Mg_{0.761}Al_{0.248}(OH)_2](CO_3)_{0.124}0.66H_2O$	3.06	8.31
MAF-10	$[Mg_{0.752}Al_{0.253}(OH)_{1.93}F_{0.07}](CO_3)_{0.126}0.58H_2O$	2.98	7.72
MAF-25	$[Mg_{0.738}Al_{0.242}(OH)_{1.73}F_{0.27}](CO_3)_{0.121}0.52H_2O$	3.04	7.59
MAF-40	$[Mg_{0.714}Al_{0.248}(OH)_{1.59}F_{0.41}](CO_3)_{0.124}0.49H_2O$	2.88	7.56

[a] As determined by chemical analysis.
[b] As determined by XRD (Lima et al., 2012.).

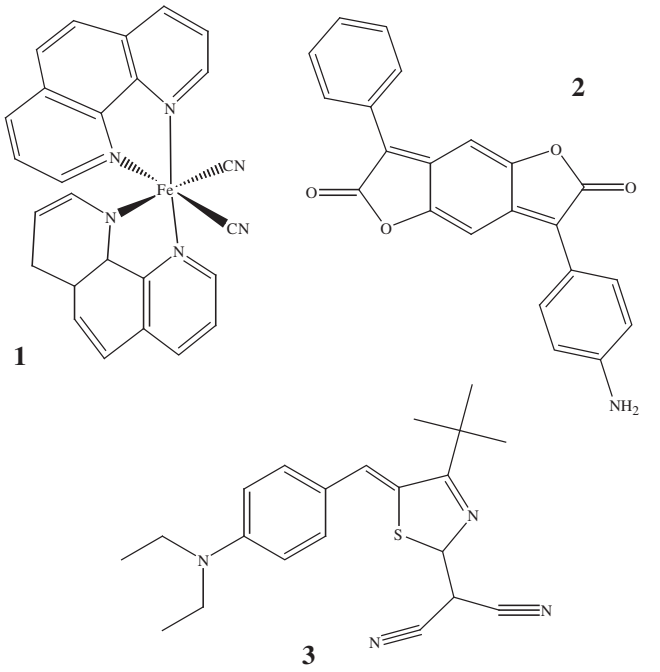

Scheme 1. Chemical structures of solvatochromic dyes.

The simplified Kamlet–Taft equation is the following:

$$\nu_{max} = \sim \nu_{max,0} + a\alpha + b\beta + s\pi^* \quad (1)$$

where $\sim\nu_{max,0}$ denotes the peak frequency value of a solvent reference system. The parameter α describes the HBD ability, β the HBA ability, and π* represents the dipolarity/polarisability. Further, a, b, and s are solvent-independent coefficients reflecting contributions of solvent effects to the UV/vis absorption shift ν_{max}. α, β, and π* can be individually derived (Spange et al., 2005) from the UV/vis absorption maxima of the perichromic probe dyes **1**–**3** (Scheme 1).

$$\alpha = -7.49 + 0.46\nu_{max}(\mathbf{1})\left[10^{-3}\mathrm{cm}^{-1}\right] \quad (2)$$

$$\beta = 3.84 - 0.20\nu_{max}(\mathbf{2})\left[10^{-3}\ \mathrm{cm}^{-1}\right] \quad (3)$$

$$\pi^* = 9.475 - 0.54\nu_{max}(\mathbf{3})\left[10^{-3}\ \mathrm{cm}^{-1}\right] \quad (4)$$

2.2.2. H_2O and CO_2–H_2O adsorption

Dynamic H_2O and CO_2–water vapour sorption experiments were carried out on a temperature controlled thermobalance TA Instruments model Q5000SA, equipped with a humidity-controlled chamber, varying temperature, time, and relative humidity. All the experiments were carried out using around 3–5 mg of thermal treated LDH, distilled water, and CO2 (Praxair, grade 3.0) as carrier gas. The CO_2 flow used was 100 mL/min, and the RH percentages were controlled automatically with the Q5000SA equipment.

2.2.3. Xenon

For these experiments, the sample was placed in a NMR tube equipped with Young valves through which the xenon gas (Praxair, 99.999%) was equilibrated with the sample at 20 °C under different pressures. Prior to xenon loading, samples were dehydrated by gradual heating up to 400 °C under vacuum (1.33×10^{-4} kPa). The ^{129}Xe NMR spectra were recorded at 20 °C using a Bruker Avance 400 spectrometer at 111.23 MHz. Single excitation pulses were used, and at least 2000

scans were collected with a delay time of 2 s. The chemical shift was referenced to xenon gas extrapolated to zero pressure.

2.2.4. Hydroxynaphthol blue

Hydroxynaphthol blue (HNB) containing LDH was obtained when 0.2 g of thermal treated LDH was put in contact with 25 mL of 5×10^{-3} M HNB solution for 5 h. Then, coloured solids where separated from colourless liquids by centrifugation and dried at 80 °C. Because the liquids were colourless after separation, it was assumed that all HNB was adsorbed by LDH.

2.3. Characterisation

The samples were characterised by X-ray diffraction (XRD), solid-state nuclear magnetic resonance (MAS NMR) of ^{27}Al and ^{13}C nuclei, thermal analysis (TGA), infrared spectroscopy (FTIR-ATR) and UV–vis spectroscopy.

The XRD patterns were acquired using a diffractometer D8 Advance-Bruker equipped with a copper anode X-ray tube. The presence of pure LDH (hydrated samples) and periclase (sample thermally activated) structures were confirmed by fitting the diffraction patterns with the corresponding Joint Committee Powder Diffraction Standards (JCPDS cards).

The single pulse solid-state ^{27}Al spectra were acquired on a Bruker Avance 300 spectrometer by using a Bruker MAS probe with a cylindrical 4 mm o.d. zirconia rotor and by operating the spectrometer at a frequency of 78.1 MHz. Short single pulses (π/12) were used. The 90° solid pulse width was 2 μs and the chemical shifts were referenced to those of an aqueous 1 M $AlCl_3$ solution. The MAS frequency was 10 kHz. All the NMR measurements were done at room temperature (20 °C).

The ^{13}C CP MAS NMR spectra were measured by operating the spectrometer at 376.3 MHz, using π/2 pulses of 6 ms with a recycle delay of 1 s.

A spectrometer Perkin-Elmer Lambda 40 was used to acquire the UV–vis powder spectra in reflection mode. Dye containing samples spectra were recorded with unmodified powders as a reference.

3. Results and discussion

3.1. Chemical composition

The chemical composition of 4 samples under study is presented in Table 1. The established nominal Mg^{2+}/Al^{3+} molar ratio was 3; the actual ratio (determined by X-ray fluorescence) varied from 2.88 to 3.06, which is within experimental error. The d_{003} distance from XRD results was included. Earlier the slight variation with the fluorine content was explained because of the strong attraction that fluorine could impose to water and anions between the layers.

3.2. Polarity and polarisability

Fig. 1 displays representative UV/vis absorption spectra of dye **1** adsorbed in the mixed oxides with or without fluoride. Spectra with a complex shape were obtained. Simple determination of the global UV/vis absorption maxima from the UV/vis absorption spectra is not adequate. Thus, with the purpose to identify the UV/vis absorption band attributable to perichromic effects, the UV/vis absorption spectra were fitted with two Gaussian components whose positions changed as a function of the samples. The component at higher wave-number was those that changed with the fluorine content, a bathochromic effect was observed: position of this component was observed at 557 nm on MA sample but it is red shifted to 573 on the sample MAF-40 sample. A second component was identified with an unchanged position at 583 ± 4 nm for all spectra. Perichromic effects are indisputably related to changes in the distribution of π electrons of dye which in turn are determined by the polarity at surface. This is surely related to fact

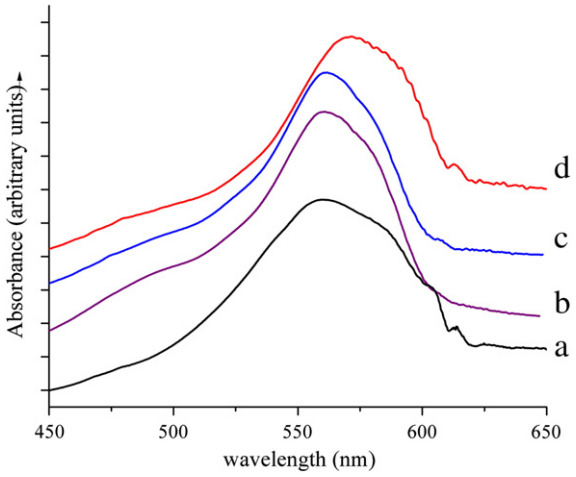

Fig. 1. UV–vis spectra of the indicator dye $Fe(phen)_2(CN)_2$ adsorbed to (a) MA, (b) MAF-10, (c) MAF-25 and (d) MAF-40.

that, as shown in our previous paper on these novel materials (Lima et al., 2012), fluorine incorporation into brucite-like layers implies that some strong basic OH are eroded, leading to surfaces with different dipole moments.

The fitting of the UV–vis absorption spectra was made for all **1**–**3** adsorbed dyes in order to identify the component of the spectra sensitive to perichromic effects. With the UV–vis absorption maxima values of these components, the Kamlet–Taft surface polarity parameters (α, β, π*) of the mixed oxide surfaces were determined by means of the well-established method (Spange et al., 2005) and using the Eqs. (2)–(4). Values of α, β and π* for the various solids are reported in Table 2.

Specific dye–surface interactions are expressed by both, the HBD and HBA abilities. Interactions of HBD surfaces with dye **1** lead to a decrease of their electron density and an increase of the push–pull character of the chromophore, thus resulting in a bathochromic UV/vis shift contribution. The HBD character of the surface is proportional to the value of α. The values of α do not differ significantly among the surfaces evaluated. Actually, only a slight decrement in the HBD ability is observed as a consequence of the fluorination of the surface. This was expected because the OH^- structural groups were replaced by F^-. It is worth emphasising that the decrease in HBD is not proportional to the fluorine content due to the dye that probes specifically the surface and not the whole structure. Thus, the density of OH^- at surface is not greatly affected by the introduction of fluoride.

Most remarkably, the β parameter increases significantly with the content of fluoride. The NH–surface interactions commonly induce a bathochromic shift in the UV/vis absorption band of the chromophore (Kamlet et al., 1983; Spange et al., 1998). HBA character of surface enhances proportionally to the fluorine content which means that the surface is fluorine enriched. This result was expected because of the ability of fluorine to form strong hydrogen bonds; additionally oxide centres have to be present at the surface. In Scheme 2 a rough model of functional chemical groups interacting with the dye probe is presented. It

Table 2
Kamlet–Taft's α, β, and π* values of mixed oxide surfaces used in this work, determined by means of dyes **1**–**3** and Eqs. (2)–(4).

Code sample	α (**1**)	β (**2**)	π*(**3**)
MA	0.74	0.23	0.90
MAF-10	0.72	0.30	1.01
MAF-25	0.69	0.42	1.10
MAF-40	0.66	0.59	1.27

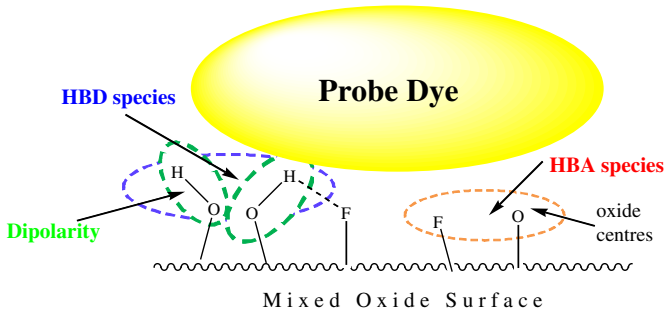

Scheme 2. Drawings that show the functional groups to be characterised at mixed oxide surfaces.

is clear that the presence of fluorine should contribute significantly to the capacity of surface to attract hydrogen atoms.

A bathochromic shift of the UV/vis absorption band of dye **3** with the increasing content of fluorine in mixed oxide was observed. Third polarity parameter, π*, represents the dipolarity/polarisability character of the surface. In the series under consideration, the bathochromic shift means that dipolarity/polarisability increases with the content of fluorine, which is not surprising because of the different dipole moments expected at the surface of solids. Turning back to Scheme 2, it can be seen that the dipole moments present at surface of Mg(Al)O mixed oxide should be seriously modified when neighbour fluorine is present. The higher electronegativity of F than O is presumably the responsible to attract the proton of OH groups creating thus a different orientation of dipole moments and modifying the disorder at surface.

In summary, probe dyes, which interact physically with surface but they can experiment chemical changes, postulate that HBA and dipolarity/polarisability are the parameters most influenced by the introduction of fluorine in mixed oxides emerged from the thermal treatment of fluorinated LDHs. In this context, xenon, an inert atomic probe, is welcomed to complement the polarisability characterisation of the surfaces. Actually, ^{129}Xe NMR has become a widely employed technique for the characterization of porous solids (Bonardet et al., 2007; Fraissard and Ito, 1988; Lima et al., 2007). Fig. 2 shows the ^{129}Xe NMR spectra of xenon adsorbed in MAF-10, the mixed oxide sample containing the lowest amount of fluorine. All spectra, independently of the amount of xenon, are composed of a single peak whose position, as expected, varies with the xenon concentration. Fig. 3 shows the effect of the amount of adsorbed xenon (Xe atoms per g of solid) on the ^{129}Xe NMR chemical shift. The chemical shift of adsorbed xenon is practically independent of the xenon concentration. This behaviour has been

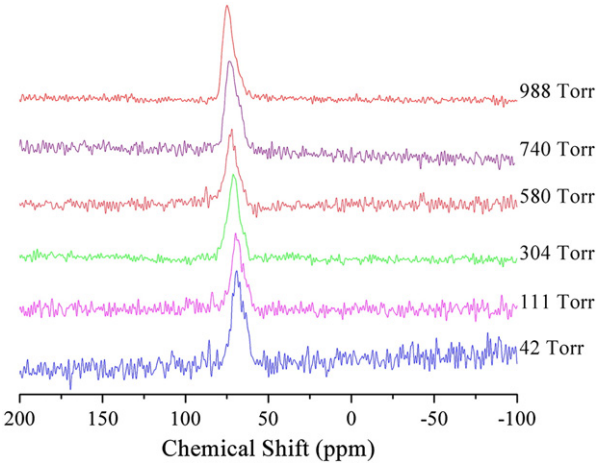

Fig. 2. ^{129}Xe NMR spectra of adsorbed xenon in MAF10 at the indicated xenon pressure.

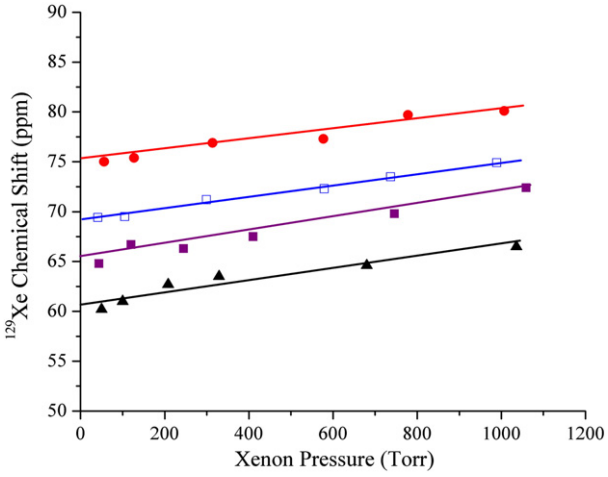

Fig. 3. ^{129}Xe chemical shift as a function of xenon in (▲) MA, (■) MAF-10, (□) MAF-25 and (●) MAF-40. The error associated to the value of chemical shift is ±0.5 ppm.

already observed in other mesoporous materials (Springuel-Huet et al., 1999; Terskikh et al., 1993) and it was explained because of the rapid exchange of the Xe in an adsorbed state in the porous and gaseous xenon in the macroporous between particles.

The observed chemical shift in the low xenon loading regime can be expressed by the following equation (Demarquay and Fraissard, 1987; Ripmeester, 1982):

$$\delta = \delta_0 + \delta_s + \sigma_{Xe}\rho \quad (5)$$

where δ and ρ denote chemical shift and xenon loading, respectively. The term δ_0 is the chemical shift reference (0 ppm). The term δ_s, which represents chemical shift at zero xenon loading, reveals interaction between Xe and the pore surfaces of the adsorbent. Lastly, the term $\sigma_{Xe}\rho$ reflects the Xe–Xe interactions that at low xenon loadings and in samples with porous ranged in the mesoporous scale are negligible. Thus, the δ_s values were calculated from Fig. 3 by extrapolating the curves to zero xenon loading. Clearly, the δ_s value of mixed oxide samples shows the expected gradual increase with the increasing fluorine content if compared to that of the parent Mg(Al)O sample. δ_s values increase proportionally to fluorine content in samples, which is interpreted as a higher polarisability of the xenon inside the pores with fluorine, in other words, the presence of fluorine induces a redistribution of dipoles inside the pores. These results are in agreement with the distribution of $MgF_{6-x}O_x$ species as a function of fluorine content as previously discussed (Lima et al., 2012; Scholz et al., 2011). Furthermore, it should be remember that the fluorine loading deeply affects the Al(IV)/Al(VI) species which again contributes to modify the polarisable character of the surface. The higher the fluorine loading the higher the Al(IV) amount species, which implies that these acid aluminium sites can act as adsorption sites for xenon.

Fig. 4 shows a linear relation between the ^{129}Xe chemical shift and the π* polarity parameter. This result is relevant as it suggests that inside the pores the adsorption sites are more versatile when fluorine is present, which often is required to design an adsorbent or a catalyst.

3.3. Adsorbate–adsorbent interactions

3.3.1. Modulation of colour in pigments

Introduction of fluorine changes significantly the physicochemical properties of LDHs, which should be relevant to both catalysis and adsorption applications. For instance, the HBD and HBA characters, influenced by the introduction of fluorine, are expected to modify the acidity as well as the basicity at the surface of materials. This fact is a

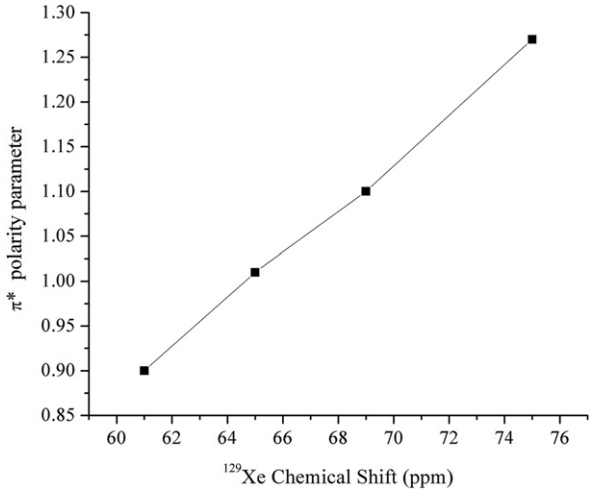

Fig. 4. Correlation of π* Kamlet–Taft parameter as a function of the ^{129}Xe chemical shift.

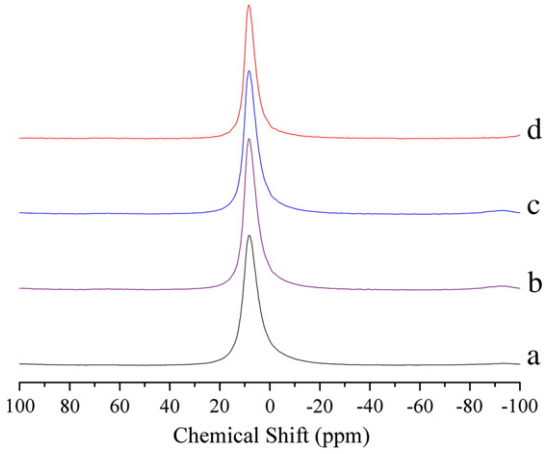

Fig. 6. ^{27}Al MAS NMR spectra of pigments composed by hydroxyl-naphthol blue adsorbed onto (a) MA, (b) MAF-10, (c) MAF-25 and (d) MAF-40.

determinant to modulate the material as an adsorbent. For instance, Fig. 5 shows the pigments emerged from the sequestering of HNB in the various mixed oxides. The samples loaded with HNB were stable at room temperature and air and they do not leach HNB when washed with water. The observed colour changes with the fluorine content in the adsorbent. With the fluorine-free sample a magenta pigment is observed but colour is enhanced when fluorine content decreases in adsorbent. HNB is well known as an indicator of the presence of Mg^{2+} because of the Mg^{2+}–HNB complex formed. Actually, the change of colour as a function of the fluorine content suggests that adsorption of HNB occurs at the $MgO_{6-x}F_x$ sites but the HNB–Mg^{2+} interaction strength is determined by the number of fluorine atoms coordinated to magnesium. The higher the number of fluorine species the lighter the colour of the pigment, which means that Mg^{2+} is better shielded by 6 fluorines than when oxygen is the first neighbouring element of magnesium, in other words some of the hardness character of Mg^{2+} is lost with the presence of fluorine. Fig. 6 displays the ^{27}Al NMR spectra of samples with HNB where no differences were observed between different samples, only an isotropic peak was observed at 8 ppm which is assigned to 6-fold coordinated aluminium. The very slight change in the peak broadness should be attributed to the presence of fluorine coordinated to aluminium rather than the HNB adsorbed. HNB is indeed used in genetic techniques (Goto et al., 2009; Zhang et al., 2011). The high sensitivity of HNB–LDH hybrid materials against polar bonds could be very useful to design sensors for application in gene amplification methods.

3.3.2. Modulating the selectivity as adsorbents

All the mixed oxides that emerged from the thermal treatment of LDH samples were rehydrated with CO_2 as a gas carrier. The adsorption–desorption isotherms were type III for all adsorbents (Fig. 7). Isotherms did not close meaning that adsorption process is irreversible; after the adsorption–desorption cycle all the samples gain weight but the amount depends of the sample composition. The weight increments are of course attributed to non-reversible structural modifications due to H_2O and/or CO_2 molecules adsorbed at surface. It is well-known that mixed oxide surfaces are easily carbonated when they are exposed to water and carbon dioxide. This carbonation is a key parameter to later reach the well-known memory effect of LDHs. It was earlier reported that the memory effect in fluorinated and fluorine-free LDHs differs, because of the electronegativity differences of fluorine and oxygen. The isotherms in Fig. 7 show the origin of the different behaviours regarding the H_2O/CO_2 adsorption. It is clear that adsorption of H_2O/CO_2 is favoured in the absence of fluorine. On the one hand, it was shown, with the adsorption of photochromic probes, that the dipole moments

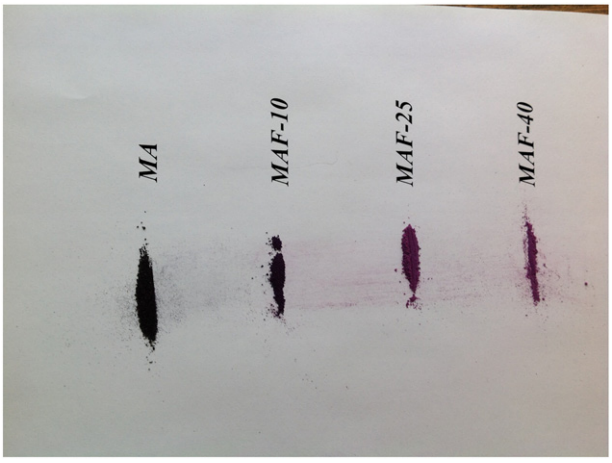

Fig. 5. Pigments obtained from stabilization of the same amount of hydroxyl-naphthol blue on different HDL supports.

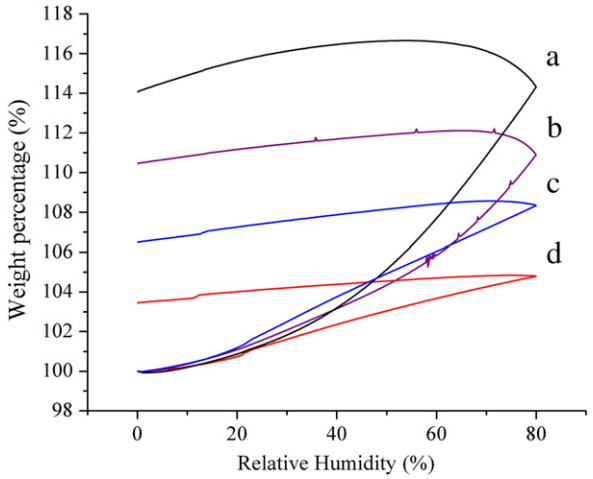

Fig. 7. Water sorption/desorption isotherms on the calcined LDH sample, generated at different temperatures using CO_2 as carrier gas. (a) MA, (b) MAF-10, (c) MAF-25 and (d) MAF-40.

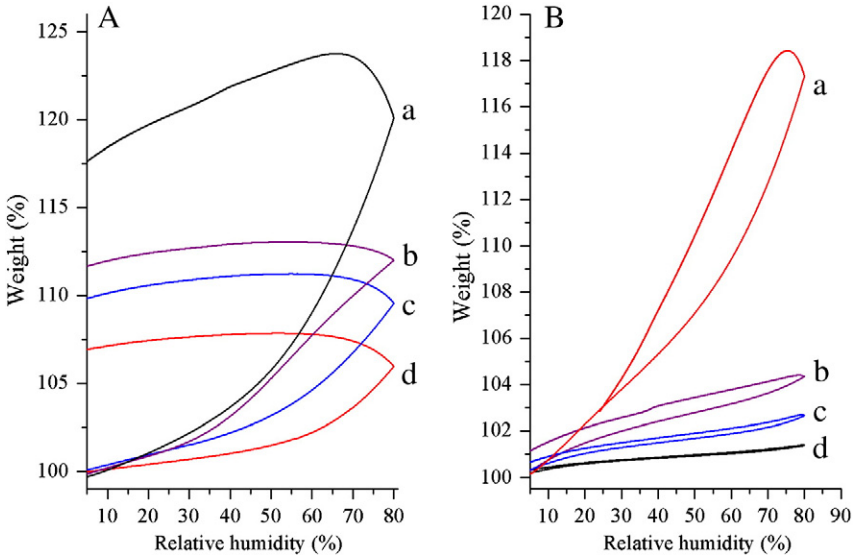

Fig. 8. Isothermal analyses of the mixed oxides (A) and hydrated hydrotalcites (B) at 60 °C in a flux of H_2O (a) MA, (b) MAF-10, (c) MAF-25 and (d) MAF-40.

are more versatile when fluorine is present and because of the electronegativity values, simply, it is expected that the strength of dipole moments in fluorinated samples tend to be higher than in free-fluorine samples. Thus, the $(dipole)_{HDL\ surface}$–$(dipole)_{H2O}$ interaction, which is proportional to the multiplication of the dipole moments, is more important in the fluorinated sample which means that the motion of water in these samples is partially restricted, leading to a slower rehydration. Furthermore, results of ^{129}Xe NMR and UV–vis spectroscopy of adsorbed dyes suggested that the polarisability and electric field gradient are enhanced with the fluorine content, thus the fluorinated samples should make dipoles easier induced in CO_2 molecules. Thus, even when more induced CO_2 dipoles should be formed and they interact with surface of mixed oxide, the strong interaction between water and surface does inhibit the CO_2 adsorption, leading to a certain phobic CO_2 character of the fluorinated hydrotalcites. This result is relevant as it opens the possibility that modifies the well-known affinity of LDHs to be carbonated. This phenomenon is hard to describe as CO_2 and H_2O were simultaneously adsorbed and the following phenomena occur: hydration of the external surface, reconstruction of the HT layered structure, and formation of various CO_2-carbonate adsorbed species. Thus, in order to better characterise the adsorption experiment, the adsorption of H_2O in the absence of CO_2 was performed. Fig. 8A displays the H_2O adsorption isotherms (60 °C), using N_2 as carrying gas, on different mixed oxide samples. Clearly, the presence of fluorine affects the H_2O adsorption behaviour, the mixed oxide fluorine-free is the solid where the water adsorption is the fastest and the sample where the highest amount of water (17.1 wt.%) is retained after desorption step. The fact that the motion of water molecules is enough to rehydrate the mixed oxide surface and begins the memory effect phenomenon is well known and explained. Interestingly, the amount of water and its adsorption rate are considerably lower in the fluorinated samples, the higher the amount of water the slower the amount of adsorbed water after the desorption process. Thus, it is confirmed that water molecules are strongly adsorbed in fluorinated surfaces, most probably on the four-fold coordinated aluminium sites. As a consequence of this strong interaction the adsorption sites are occupied for longer periods inhibiting then the adsorption process even for other molecules like CO_2. When the water adsorption was made on the hydrated samples, the dynamic of adsorption–desorption process was dramatically inhibited by the presence of fluorine (Fig. 8B). In the fluorine-free sample, the amount of adsorbed water, varying the relative humidity, can be as high as 20 wt.% but in the sample with the highest amount of fluorine the maximum of adsorbed water is only 7 wt.%. In these experiments, the water is mainly adsorbed onto the surface of solid, therefore it is clear that the fluorination of HTs changes their properties at external surface as well as into the porous as supported by CO_2 dyes and xenon adsorption.

4. Conclusion

Fluorination of the brucite-like layers of layered double hydroxides changes significantly their adsorption properties. Hydrogen bond donating character of solids is almost unaltered by the presence of *fluorine*; on the contrary, hydrogen bond accepting character is significantly enhanced. Polarity and polarisability are two parameters that are also enhanced with the presence of fluorine because of the versatility of the dipolar moments and their distribution at surface. The changes in the physicochemical parameters at the surface of LDHs modify greatly their adsorption properties. For instance, the fluorinated samples are suitable to create stable pigments and adsorbents that show resistance to be carbonated.

Acknowledgments

The authors would like to acknowledge CONACYT for Grant 128299. We are grateful to G. Cedillo and A. Tejeda for the technical assistance. E. Lima acknowledges PASPA UNAM programme for financial support.

References

Beaudot, P., De Roy, M.E., Besse, J., 2004. Preparation and characterization of intercalation compounds of layered double hydroxides with metallic oxalato complexes. Chem. Mater. 16 (5), 935–945.
Bonardet, J., Gédeon, A., Springuel-Huet, M.-A., Fraissard, J., 2007. In: Karge, H.G., Weitkamp, J. (Eds.), Molecular Sieves, Characterization II. Springer, New York, pp. 155–248.
Cheng, J., Wang, X., Yu, J., Hao, Z., Xu, Z.P., 2011. Sulfur-resistant NO decomposition catalysts derived from Co–Ca/Ti–Al hydrotalcite-like compounds. J. Phys. Chem. C 115 (14), 6651–6660.
Costantino, U., Coletti, N., Nocchetti, M., Aloisi, G.G., Elisei, F., 1999. Anion exchange of methyl orange into Zn–Al synthetic hydrotalcite and photophysical characterization of the intercalates obtained. Langmuir 15 (13), 4454–4460.
Demarquay, J., Fraissard, J., 1987. ^{129}Xe NMR of xenon adsorbed on zeolites: relationship between the chemical shift and the void space. Chem. Phys. Lett. 136 (3–4), 314–318.
Duan, X., Evans, D.G., 2006. In Layered Double Hydroxides. Springer-Verlag, Berlin-Heidelberg, Germany.
Fraissard, J., Ito, T., 1988. ^{129}Xe n.m.r. study of adsorbed xenon: a new method for studying zeolites and metal-zeolites. Zeolites 8 (5), 350–361.
Goto, M., Honda, E., Ogura, A., Nomoto, A., Hanaki, K., 2009. Colorimetric detection of loop-mediated isothermal amplification reaction by using hydroxy naphthol blue. Biotechniques 46 (3), 167–172.

Hattori, H., 1995. Heterogeneous basic catalysis. Chem. Rev. 95, 537–550.
Hibino, T., Tsunashima, A., 1998. Characterization of repeatedly reconstructed Mg–Al hydrotalcite-like compounds: gradual segregation of aluminum from the structure. Chem. Mater. 10 (12), 4055–4061.
Kamlet, M.J., Abboud, J.-S.M., Abraham, M.H., Taft, R.W., 1983. Linear solvation energy relationships. 23. A comprehensive collection of the solvatochromic parameters, pi.*, alpha., and .beta., and some methods for simplifying the generalized solvatochromic equation. J. Org. Chem. 48 (17), 2877–2887.
Katritzky, A.R., Fara, D.C., Yang, H., Tämm, K., Tamm, T., Karelson, M., 2004. Quantitative measures of solvent polarity. Chem. Rev. 104, 175–198.
Laguna, H., Loera, S., Ibarra, I.A., Lima, E., Vera, M.A., Lara, V., 2007. Azoic dyes hosted on hydrotalcite-like compounds: non-toxic hybrid pigments. Microporous Mesoporous Mater. 98 (1–3), 234–241.
Lima, E., Balmaseda, J., Reguera, E., 2007. ^{129}Xe NMR spectroscopy study of porous cyanometallates. Langmuir 23 (10), 5752–5756.
Lima, E., Martínez-Ortiz, M.J., Gutiérrez-Reyes, R.I., Vera, M., 2012. Fluorinated hydrotalcites: the addition of highly electronegative species in layered double hydroxides to tune basicity. Inorg. Chem. 51 (14), 7774–7781.
Lungwitz, R., Spange, S., 2008. A hydrogen bond accepting (HBA) scale for anions, including room temperature ionic liquids. New J. Chem. 32 (3), 392–394.
Martínez-Ortiz, M.J., Lima, E., Lara, V., Méndez Vivar, J., 2008. Structural and textural evolution during folding of layers of layered double hydroxides. Langmuir 24 (16), 8904–8911.
Miyata, S., 1975. The syntheses of hydrotalcite-like compounds and their structures and physico-chemical properties I: the systems Mg^{2+}–Al^{3+}–NO_3^-, Mg^{2+}–Al^{3+}–Cl^-, Mg^{2+}–Al^{3+}–ClO_4^-, Ni^{2+}–Al^{3+}–Cl^- and Zn^{2+}–Al^{3+}–Cl^-. Clays Clay Miner. 23 (5), 369–375.
Occelli, M.L., Olivier, J.P., Auroux, A., Kalwei, M., Eckert, H., 2003. Basicity and porosity of a calcined hydrotalcite-type material from nitrogen porosimetry and adsorption microcalorimetry methods. Chem. Mater. 15 (22), 4231–4238.
Perioli, L., Posati, T., Nocchetti, M., Bellezza, F., Costantino, U., Cipiciani, A., 2011. Intercalation and release of antiinflammatory drug diclofenac into nanosized ZnAl hydrotalcite-like compound. Appl. Clay Sci. 53 (3), 374–378.
Pfeiffer, H., Lima, E., Lara, V., Valente, J.S., 2010. Thermokinetic study of the rehydration process of a calcined MgAl-layered double hydroxide. Langmuir 26 (6), 4074–4079.
Ripmeester, J.A., 1982. Nuclear shielding of trapped xenon obtained by proton-enhanced, magic-angle spinning xenon-129 NMR spectroscopy. J. Am. Chem. Soc. 104 (1), 289–290.
Sampieri, A., Lima, E., 2009. On the acid–base properties of microwave irradiated hydrotalcite-like compounds containing Zn^{2+} and Mn^{2+}. Langmuir 25 (6), 3634–3639.
Scholz, G., Stosiek, C., Noack, J., Kemnitz, E., 2011. Local fluorine environments in nanoscopic magnesium hydr(oxide) fluorides studied by ^{19}F MAS NMR. J. Fluorine Chem. 132 (12), 1079–1085.
Seifert, S., Seifert, A., Brunklaus, G., Hofmann, K., Ruffer, T., Lang, H., Spange, S., 2012. Probing the surface polarity of inorganic oxides using merocyanine-type dyes derived from barbituric acid. New J. Chem. 36 (3), 674–684.
Spange, S., Reuter, A., Vilsmeier, E., Heinze, T., Keutel, D., Linert, W.J., 1998. Determination of Empirical polarity parameters of the cellulose solvent N. N-dimethylacetamide/LiCl by means of the solvatochromic technique. Polym. Sci., Part A: Polym. Chem. 36 (11), 1945–1955.
Spange, S., Zimmermann, Y., Graeser, A., 1999. Hydrogen-bond donating acidity and dipolarity/polarizability of surfaces within silica gels and mesoporous MCM-41 materials. Chem. Mater. 11 (11), 3245–3251.
Spange, S., Schmidt, C., Kricheldorf, H.R., 2001. Probing the surface polarity of poly(α-amino acids) and α-amino acid crystals with genuine solvatochromic dyes. Langmuir 17 (3), 856–865.
Spange, S., Prause, S., Vilsmeier, E., Thiel, W.R., 2005. Probing surface basicity of solid acids with an aminobenzodifurandione dye as the solvatochromic probe. J. Phys. Chem. B 109 (15), 7280–7289.
Springuel-Huet, M.-A., Sun, K., Fraissard, J., 1999. On the roughness of the internal surface of MCM-41 materials studied by ^{129}Xe NMR. Microporous Mesoporous Mater. 33 (1–3), 89–95.
Stanimirova, T.S., Vergilov, I., Kirov, G., Petrova, N., 1999. Thermal decomposition products of hydrotalcite-like compounds: low-temperature metaphases. J. Mater. Sci. 34 (17), 4153–4161.
Terskikh, V.V., Mudrakovskii, I.L., Mastikhin, V., 1993. ^{129}Xe nuclear magnetic resonance studies of the porous structure of silica gels. J. Chem. Soc., Faraday Trans. I 89 (23), 4239–4243.
Xu, Z.P., Zeng, H.C., 2001. Decomposition pathways of hydrotalcite-like compounds $Mg_{1-x}Al_x(OH)_2(NO_3)_x \times nH_2O$ as a continuous function of nitrate anions. Chem. Mater. 13 (12), 4564–4572.
Zhang, Y., Fu, P., Li, J., Jiang, F., Li, J., Wu, W., 2011. Development of loop-mediated isothermal amplification method for visualization detection of the highly virulent strains of porcine reproductive and respiratory syndrome virus (PRRSV) in China. Afr. J. Biotechnol. 10 (61), 13278–13283.
Zimmermann, Y., Anders, S., Hofmann, K., Spange, S., 2002. Influence of chemical solvent properties on the external and internal surface polarity of silica particles in slurry. Langmuir 18 (24), 9578–9586.